Capacitance in open quantum structures

P. N. Racec,* E. R. Racec,† and Ulrich Wulf
Technische Universität Cottbus, Fakultät 1, Postfach 101344, 03013 Cottbus, Germany
(Received 18 March 2002; published 10 May 2002)

Opposite to the well-known statistical limit, we study a semiconductor quantum system with only one relevant resonance which is in contact with a probe acting as a particle reservoir. We find that the quasibound state that exists in the nearly closed system develops at a transition to the open system into a separate type of resonance. In contrast to the quasibound state (i) it is localized in the space between the probe and the isolated quantum system, (ii) its energy lies in the classically allowed regime, and (iii) its line shape is strongly asymmetric. Excellent quantitative agreement shows that this transition is seen in capacitance experiments on MIS (metal-insulator-semiconductor)-type semiconductor heterostructures in which a field-induced two-dimensional electron gas is formed.

DOI: 10.1103/PhysRevB.65.193314 PACS number(s): 73.23.Ad, 73.40.Kp, 73.40.Qv, 73.63.Hs

The rapid progress in semiconductor technology has led to a great variety of different semiconductor quantum structures in which a wide spectrum of interesting effects have been observed.[1] In recent research on the Kondo effect,[2] on fluctuations of the local density of states in the emitter[3] and on Luttinger liquid behavior in ballistic transport through quantum wires,[4] the importance of the interaction of the quantum system with the contacts has been established. Here we perform a microscopic study of this interaction emphasizing the importance of the coupling of the isolated quantum system (QS) to contacts through particle exchange. Generally, the character of the resulting electronic states depends critically on the number of the relevant resonances in the QS, on the number of channels in the probes to which the resonances couple, and on the strength of this coupling. Using a statistical approach, very successful and well-known work has been devoted to the case of many resonances which couple to a number of channels:[5] at weak coupling of the QS to the probes, the resulting narrow Coulomb blockade peaks show a statistical behavior of the peak height. At strong coupling the levels widen, and their superposition leads to a conductance with statistical fluctuations.

Here we consider a structure in which the entire transition from weak to strong coupling can be examined experimentally and theoretically. This transition, however, occurs in the opposite limit, i.e., there is only a single relevant resonance and there is no channel mixing. As expected, in the weak-coupling regime the bound state of the QS turns into a narrow quasibound state (QBS) with nearly identical location in space. We find that with increasing coupling the QBS turns into an ''intermediate resonance'' (IR). In contrast to the QBS the IR has the following properties: First, it is located in the space between the probes and the isolated QS. Second, in difference to the case of the QBS which is coupled to the probes only via the tunneling effect the IR occurs in the open system where there is a channel of classically allowed motion (see the shaded area in the lower part of Fig. 2). Third, since the decay of the IR into the probe is classically allowed it has the character of a Fabry-Perot resonance. Fourth, the IR is strongly asymmetric, and can well be described by a Fano distribution with a complex asymmetry parameter. Finally, if the coupling becomes too strong a resonant state cannot exist any longer. Because of the excellent quantitative agreement with our theory we can demonstrate that the transition between QBS and IR is directly seen in capacitance experiments by Dolgopolov *et al.*:[6] In this structure the QS is a field-induced two-dimensional electron gas (2DEG). The step in the C-V characteristic associated with its formation (see upper part of Fig. 2) is broadened because of the energetic overlapping of the channel of allowed classical motion and the IR. In our calculations the classically allowed channel in which the IR exists only results when the Coulomb interaction between the electrons is taken into account, at least in the self-consistent mean-field approximation. Therefore, in the absence of similar self-consistent calculations for open systems with many pertinent resonances, we cannot make a statement as to whether in these systems a IR is formed. The considered AlAs/GaAs MIS (metal-insulator-semiconductor)-type heterostructure (see Fig. 1), consists of a sequence of layers grown on a $GaAs$ bulk material given by, (i) n-GaAs as a back contact, (ii) intrinsic GaAs as a spacer, (iii) a short period $Al_xGa_{1-x}As$/GaAs superlattice as a blocking barrier, (iv) a GaAs cap layer, and finally a metallization as a top gate. Also shown in Fig. 1 is the band structure taken from a self-consistent calculation according to Eqs. (1)–(3). These calculations show that, with an increasing positive gate voltage V_G, a triangular-shaped potential quantum well is progressively formed at the interface $(z=z_b)$ between the GaAs spacer and the blocking barrier, in which the electrons accumulate. At large enough voltages a 2DEG is formed when the coupling to the contacts become negligible.

Because of the translational invariance of our system in the lateral directions, the standard envelope-function approximation, for a conduction electron with the total energy E, yields the Schrödinger equation in the growth direction,

$$\left[-\frac{\hbar^2}{2m^*}\frac{d^2}{dz^2}+V(z)-\epsilon\right]\psi^{(s)}(\epsilon,z)=0, \tag{1}$$

with $\epsilon=E-\hbar^2(k_x^2+k_y^2)/(2m^*)$. For the one-dimensional scattering potential $V(z)$ we assume $V(z<-d)=V_1$ and $V(z>d)=V_2$. For total energies larger than V_1 and V_2 there are two linearly independent solutions, so that $s=1$ and 2. We choose $\psi^{(1)}$ as a left-incident scattering function with the asymptotic $\psi^{(1)}(\epsilon,z<-d)=\exp(ik_1z)+r_1\exp(-ik_1z)$ and

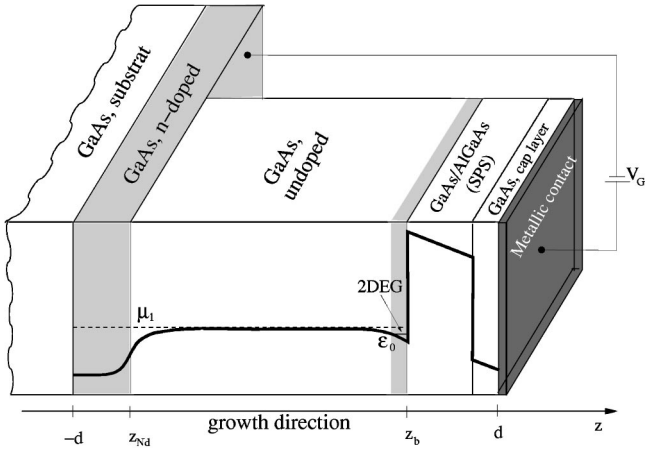

FIG. 1. The AlAs/GaAs MIS-type heterostructure. Band diagram taken from a self-consistent calculation with parameters corresponding to the experiments in Ref. 6: $-d-z_{Nd}=20$ nm, $z_b-z_{Nd}=100$ nm, a width of the cap layer of 9 nm, a width of the blocking barrier of 32 nm, an effective mass $m^*=0.066m_0$, $\kappa_{GaAs}=\kappa_{AlGaAs}=12.5\varepsilon_0$, $N_D-N_A=4\times10^{18}$ cm^{-3} for $z<z_{Nd}$, and $N_A-N_D=10^{15}$ cm^{-3} for $z_{Nd}<z<d$, where N_D and N_A are the concentrations of the ionized donors and acceptors, respectively.

$\psi^{(1)}(\epsilon,z>d)=t_1\exp(ik_2z)$, where $k_s=\sqrt{2m^*(\epsilon-V_s)/\hbar^2}$. Likewise, $\psi^{(2)}$ is selected as a right-incident scattering function. The total potential $V(z)$ is the sum of (i) the fixed potential of the band offsets in the heterostructure, $V_h(z)$, and (ii) the potential of the ionized impurities; together with (iii) the potential of the electron-electron interaction which we take in the Hartree approximation, yielding the total Coulomb potential $V_c(z)$. For the donors $N_D(z)$ in the n-GaAs and the natural acceptors $N_A(z)$ in the spacer layer we assume complete ionization and homogeneous distribution. $V_c(z)$ then satisfies the equation

$$\frac{d^2V_c(z)}{dz^2}=\frac{e^2}{\epsilon_0\epsilon_r}[N_D(z)-N_A(z)-\rho(z)], \tag{2}$$

with the boundary conditions determined by the external electric field, $V_c(-d)=0$ and $V_c(d)=\mu_1-eV_G+e\Phi_{Bn}$. $e\Phi_{Bn}$ is the barrier height of (gate) metal-semiconductor contact and V_G is the applied bias between back contact and top gate. To find $\rho(z)$ we apply the Landauer-Büttiker picture[7] in which the occupation of each scattering state is given by the Fermi function $f_{FD}(E-\mu_s)$. Here μ_s is the chemical potential in the back gate ($s=1$) or in the top gate ($s=2$). It results that

$$\rho(z)=\sum_{s=1,2}\int dE\,\frac{D(E)}{4\pi^2}f_{FD}(E-\mu_s)|\psi^{(s)}(\epsilon,z)|^2, \tag{3}$$

where $D(E)$ is the 3D density of incident states. The blocking barrier is now assumed to suppress charge transfer completely, and we consider the limit of small frequencies. Then the tunnel capacitor in Fig. 1 becomes equivalent to a simple plate capacitor.[8] The charge corresponding to the left plate is distributed in the region $-d<z<z_b$ (see Fig. 1) and can be evaluated using Gauss' law, $Q_L=-S\kappa(\partial V/\partial z)(z=z_b)$. Here S is the area of the sample, and κ is the dielectric permittivity. The top gate of the structure acts as the right plate of the capacitor and the charge on it is $Q_R=-Q_L$. The capacitance is then readily found as $C=(\partial Q_R/\partial V_g)$.

The upper part of Fig. 2 shows in comparison the experimental data[6] and the results of our numerical calculations for the step in the C-V curve associated with the formation of the 2DEG. This step is broadened and located between a low-voltage plateau, $V<V_-$, and a high-voltage plateau, $V>V_+$, both with a weak positive slope. We define the gate voltage V_c at the center of the step through the condition $d^2C/dV_g^2=0$, and V_- and V_+ correspond to the gate voltages where $|dC/dV_g|$ takes half of its maximum value. We emphasize the excellent quantitative agreement between theory and experiment, which shows that the Hartree approximation provides a very good mean-field description of the electron-electron interaction for this system.

From Fig. 2 it can be seen that the step in the C-V characteristic is located in a regime of gate voltages where the maximum V_{max} of the potential barrier which separates the probe from the potential quantum well at $z=z_b$ is below the chemical potential μ_1 in the back contact. Consequently there is an open channel of classically allowed motion: $V_{max}<\epsilon<\mu_1$. This finding resulted in a number of calculations with varying distance of the back gate to the barrier, and varying background doping concentrations in the GaAs-spacer layer.

To analyze the physical process that underlies the step in the C-V curve, in Fig. 3 we plot the energy and space dependences of the probability distribution density, $P_\epsilon(z)=|\psi^{(1)}(\epsilon,z)|^2$, to find an electron in the state $\psi^{(1)}(\epsilon,z)$ in a volume element at the given z coordinate. In the low-voltage

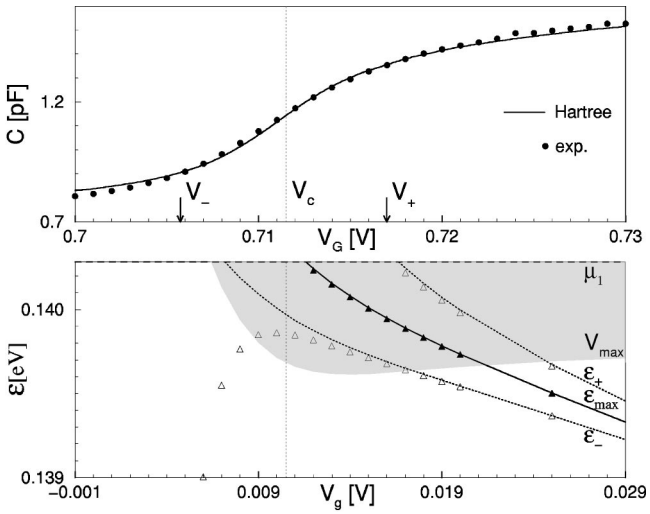

FIG. 2. Upper part: The C-V curve, experimental data (Ref. 6) (filled circles), and theory (solid line). Because the work function of the metal contact is not known precisely, we shift the theoretical voltage scale V_g with respect to the experimental one V_G, so that the centers of the steps coincide. Lower part: As the result of the complete numerical calculation the resonance energy ϵ_{max} (solid line), and the energies $\epsilon_\pm$ (dotted lines; see the text). The corresponding values ϵ^F_{max} (filled triangle) and $\epsilon^F_\pm$ (triangle) in the Fano approximation [Eq. (8)]. Shaded area: energies with $V_{max}<\epsilon<\mu_1$.

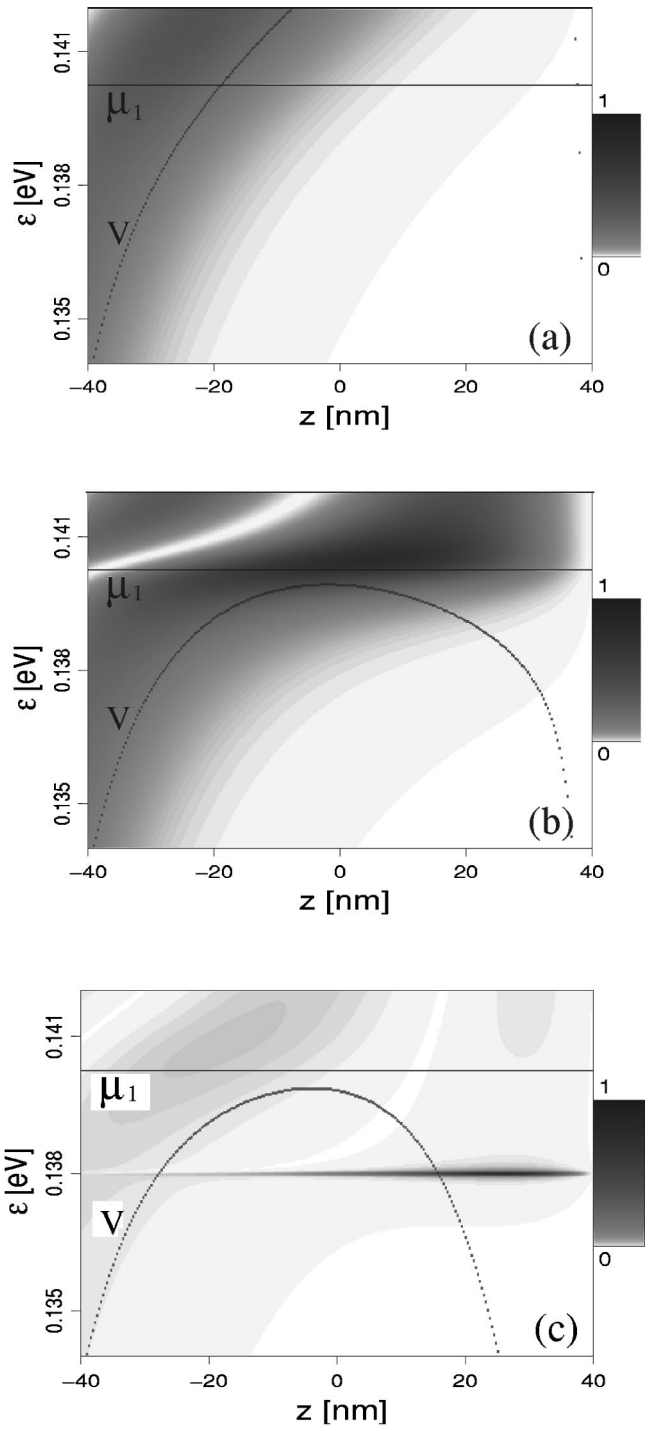

FIG. 3. The electron probability distribution density $P_\epsilon(z)/P_{max}$ with $[V_g$ (V); ϵ_{max} (eV); z_{max} (nm); z_0 (nm)], where z_0 is the position of V_{max} (a) Low voltage plateau, (-0.005,-,-,-,). (b) Center of the capacitance step (0.0105, 0.1405, 7, −2). (c) High voltage plateau (0.06, 0.138, 27.5, −3.8). P_{max} it depends on the applied voltage V_g. Note that $z_{Nd}=-60.5$ nm, $z_b=39.5$ nm, and $d=80.5$ nm.

plateau [Fig. 3(a)] the wave functions are confined in the back contact (apart from an exponential decay outside). There is no particular energy structure of the scattering functions. In contrast, in the center of the step, around V_c [Fig. 3(b)] there is a pronounced maximum P_{max} of P at $\epsilon=\epsilon_{max}$ and $z=z_{max}$ which defines the IR. The resonance energy lies in the classically allowed range and the IR thus has a Fabry-Perot character. The spatial center of the IR, z_{max}, is close to the place $z=z_0$ of the potential maximum i.e., the IR is located in the space between the probe and the potential quantum well in which the isolated 2DEG is formed at higher voltages. Finally, in the high-voltage plateau [Fig. 3(c)] the resonance corresponds to a QBS. Because of the weak penetration of the wave functions into the back contact, the lifetime of this resonance becomes large and its width narrows considerably. Furthermore, z_{max} is located in the middle of the potential quantum well of the 2DEG.

In the lower part of Fig. 2 we show ϵ_{max} and the energies $\epsilon_\pm$ at which the probability distribution density takes half its maximum value, $P_{\epsilon_{max}}(z_{max})$, at constant $z=z_{max}$ (see Fig. 3). It is seen that the center of the step in the C-V trace nearly coincides with the gate voltage at which $\epsilon_{max}=\mu_1$. Furthermore, the voltage V_- occurs roughly at $\epsilon_-=\mu_1$, and the onset of the high-voltage plateau V_+ can be associated with $\epsilon_+=\mu_1$. This confirms the view that the capacitance step is dominated by the IR: At no coupling to the probes one would expect a jump in the capacitance which occurs if the chemical potential in the back contact reaches a new energy level of the QS. Instead, in the open system one sees a gradual increase of the capacitance in the voltage regime between V_- and V_+ whose width is determined to a great extent by the energetic width of the IR.

To demonstrate further that the step in the C-V characteristic and the subsequent high-voltage plateau are dominated by a single resonance which changes its character from a IR to a QBS, we apply our resonance theory in Ref. 9 which is basically equivalent to the effective non-Hermitian Hamiltonian method for open systems.[5,10] As an advantage, our reformulation permits a convenient separation of the singular part in the S matrix, thus allowing for a systematic linearization of the problem for quasi-isolated resonances: in the energy interval in which a given resonance with the label λ extends, the scattering functions can be written as

$$\psi^{(s)}(\epsilon,z)=\frac{Z^{(s)}(\epsilon,z)}{\epsilon-\epsilon_\lambda-\overline{\mathcal{E}_\lambda}(\epsilon)}. \tag{4}$$

The functions $Z^{(s)}$ and $\overline{\mathcal{E}_\lambda}$ are directly related to the wave vector matrix, $\mathbf{K}_{ss'}=k_s\delta_{ss'}$, and to the R matrix whose elements are defined as

$$R(z,z')=\sum_l^\infty \frac{\beta_l(z,z')}{\epsilon-\epsilon_l}=R_\lambda(z,z')+\frac{\beta_\lambda(z,z')}{\epsilon-\epsilon_\lambda}, \tag{5}$$

with $\beta_l(z,z')=\chi_l(z)\chi_l(z')$. The real Wigner-Eisenbud functions χ_l and energies ϵ_l are the solutions of the 1D Schrödinger equation (1) with the homogeneous von Neumann boundary conditions at $z=\pm d$. We define further the 2×2 matrix $\mathbf{\Omega}=\mathbf{K}^{1/2}\mathbf{R}\mathbf{K}^{1/2}$, where $\mathbf{R}_{ss'}=R[(-1)^s d,(-1)^{s'} d]$, and split it, similar to the R matrix, into two parts: $\mathbf{\Omega}=\mathbf{\Omega}_\lambda+\boldsymbol{\omega}_\lambda/(\epsilon-\epsilon_\lambda)$ [see Eq. (5)]. With these notations the functions in Eq. (4) can be written as

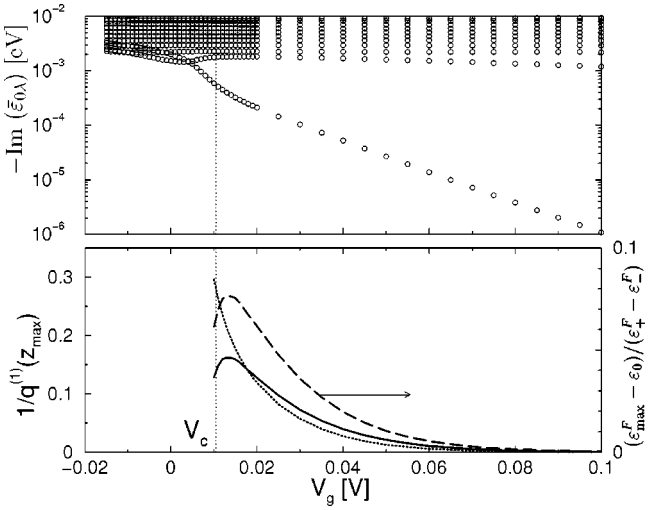

FIG. 4. Upper part: The imaginary part of $\bar{\epsilon}_{0\lambda}$ (see the text) vs the gate voltage V_g. Lower part: real part (solid line) and imaginary part (dotted line) of the complex asymmetry parameter $1/q^{(1)}(z_{max})$, and the deviation of the maximum of the Fano distribution from the pole energy ϵ_0 (dashed line) at gate voltages $V_g > V_c$.

$$\bar{\mathcal{E}}_\lambda(\epsilon) = -i\,\mathrm{Tr}[\boldsymbol{\omega}_\lambda(\mathbf{1}+i\boldsymbol{\Omega}_\lambda)^{-1}] \tag{6}$$

and inside the scattering region ($|z|<d$) as

$$\begin{pmatrix} Z^{(1)}(\epsilon,z) \\ Z^{(2)}(\epsilon,z) \end{pmatrix} = \frac{2i\Theta}{\sqrt{2\pi}}\mathbf{K}^{1/2}\frac{[\mathbf{1}+i\boldsymbol{\Omega}^-](\epsilon-\epsilon_\lambda)}{\det[\mathbf{1}+i\boldsymbol{\Omega}_\lambda]}$$

$$\mathbf{K}^{1/2}\begin{pmatrix} R(-d,z) \\ R(+d,z) \end{pmatrix}, \tag{7}$$

where $\Theta_{ss'}=\theta(\epsilon-V_s)\,\delta_{ss'}$ and $\boldsymbol{\Omega}^- = \boldsymbol{\Omega}^{-1}\det\boldsymbol{\Omega}$. From general theory[11] it follows that the resonance λ corresponds to a pole $\bar{\epsilon}_{0\lambda}$ of the S matrix in the complex energy plane. Using Eq. (4) we find the condition $\bar{\epsilon}_{0\lambda}-\epsilon_\lambda-\bar{\mathcal{E}}_\lambda(\bar{\epsilon}_{0\lambda})=0$. The upper part of Fig. 4 shows the imaginary part of the poles closest to the real axis in dependence on the gate voltage. It is clearly seen that at the end of the low-voltage plateau a single pole becomes separated from all other resonances. For simplicity we denote it with $\lambda=0$ and the associated complex energy with $\bar{\epsilon}_{00}=\epsilon_0-i\Gamma/2$. For gate voltages larger than V_c this pole corresponds to a narrow resonance, so that in its vicinity the functions $Z^{(s)}(\epsilon,z)$ and $\bar{\mathcal{E}}_\lambda(\epsilon)$ can be linearized and one obtains for the wave functions at a fixed z a Fano distribution,

$$\psi^{(s)}(\epsilon,z) \simeq i\psi^{(s)}(\epsilon_0,z)\frac{\frac{1}{q^{(s)}(z)}e+1}{e+i} \tag{8}$$

with a complex asymmetry parameter

$$\frac{1}{q^{(s)}(z)} = \frac{\Gamma/2}{Z^{(s)}(\epsilon_0,z)}\frac{d}{d\epsilon}Z^{(s)}(\epsilon,z)\big|_{\epsilon=\epsilon_0}, \tag{9}$$

where $e=2(\epsilon-\epsilon_0)/\Gamma$. We plot in the lower part of Fig. 2 the energy ϵ^F_{max} of the maximum of $|\psi^{(1)}(\epsilon,z_{max})|^2$ calculated in the linearized theory [Eq. (8)]. Furthermore, we include the energies $\epsilon^F_\pm$ at which the absolute of the Fano function takes half its maximum value at constant $z=z_{max}$. For voltages larger than V_c there is an excellent agreement between ϵ^F_{max} and $\epsilon^F_\pm$ and their counterparts ϵ_{max}, $\epsilon_\pm$ resulting from the complete numerical calculation. In the lower part of Fig. 4 we plot the real and the imaginary part of $1/q^{(1)}$ at $z=z_{max}$. For gate voltages in the step region both quantities are large and cause a distinct separation of ϵ_0 (real part of the pole) and ϵ^F_{max}. With increasing voltage the asymmetry decreases to become negligible in the high-voltage plateau, and Eq. (8) provides a Breit-Wigner distribution with the symmetry center given by ϵ_0 for $P_\epsilon(z)$.

To summarize, we find and characterize a resonance which we call the intermediate resonance and which results from a quasibound state when the coupling to external contacts is increased.

We thank W. Hansen and J. Kučera for highly valued discussions. We also thank V.T. Dolgopolov for providing the original experimental data.

*National Institute R&D of Materials Physics, PO Box MG-7, 76900 Bucharest Magurele, Romania.
†University of Bucharest, Faculty of Physics, PO Box MG-11, 76900 Bucharest Magurele, Romania.

[1] *Mesoscopic Physics and Electronics*, edited by T. Ando, Y. Arakawa, K. Furuya, S. Komiyama, and H. Nakashima (Springer, Berlin, 1998).
[2] D. Goldhaber-Gordon, J. Göres, M.A. Kastner, Hadas Shtrikman, D. Mahalu, and U. Meirav, Phys. Rev. Lett. **81**, 5225 (1998).
[3] T. Schmidt, P. König, E. McCann, Vladimir I. Fal'ko, and R.J. Haug, Phys. Rev. Lett. **86**, 276 (2001).
[4] S. Lal, S. Rao, and D. Sen, Phys. Rev. Lett. **87**, 026801 (2001).
[5] A review article can be found in Y. Alhassid, Rev. Mod. Phys. **72**, 895 (2000).
[6] V.T. Dolgopolov, A.A. Shashkin, A.V. Aristov, D. Schmerek, H. Drexler, W. Hansen, J.P. Kotthaus, and M. Holland, Phys. Low-Dim. Struct. **6**, 1 (1996).
[7] M. Büttiker, Phys. Rev. B **38**, 9375 (1988); I. Imry and R. Landauer, Rev. Mod. Phys. **71**, S306 (1999).
[8] R.E. Cavicchi and R.H. Silsbee, Phys. Rev. B **37**, 706 (1988).
[9] E. R. Racec and U. Wulf, Phys. Rev. B **64**, 115318 (2001).
[10] P. Šeba, Phys. Rev. B **53**, 13024 (1996).
[11] I. Kukulin, M. Krasnopolsky, and J. Horacek, *Theory of Resonances: Principles and Applications* (Kluwer, Dordrecht, 1989).